Production Engineering (2019) 13:399–407
https://doi.org/10.1007/s11740-019-00886-3

PRODUCTION PROCESS

Laser shock punching: principle and influencing factors

H. Fenske[1] · **F. Vollertsen**[1,2]

Received: 18 September 2018 / Accepted: 21 January 2019 / Published online: 7 February 2019

Abstract
Laser shock punching is a novel shearing process, which utilizes the pressure of pulsed TEA-CO_2 laser-induced shock waves to cut foils in the micrometre range. Thin foils are difficult to cut with conventional shearing processes, because the cutting clearance scales with the foil thickness. By using a shock wave instead of a punch to transmit the cutting force, the cutting clearance ceases to exist. In order to realise single pulse cutting, certain requirements have to be met. On the one hand it is compulsory to produce high enough operating pressures. On the other hand the cutting edge still has to be "sharp" relatively to the only micrometre thick foils. If those requirements are fulfilled, the maximum cuttable foil thickness correlates with the geometrical ratio of pressurized area to cutting path length, which can roughly be described via a balance of forces between the applied force via pressure and the required force for cutting. For foils in the micrometre range size effects have to be considered. Apart from the already mentioned challenges with the geometrical scaling of the cutting edge, single grain effects are relevant for laser shock punching. If the grain size is in the range of the foil thickness, only incomplete cutting can be realised as the foil tends to rupture within the pressurized area and the cut edge exhibits an increased and inhomogeneous burr formation. Based on the identified influencing factors, the possibilities and process limits of laser shock punching can be evaluated.

Keywords Laser shock punching · Micro punching · High speed punching · Laser-induced shock wave

1 Introduction

The general trend for miniaturisation makes it necessary to use manufacturing processes in ever smaller dimensions. Single-stroke shearing is an economically as well as ecologically attractive process for sheet metal processing and accordingly the miniaturisation of this process is actively researched. However, if conventional manufacturing processes are simply scaled down, size effects do occur [1] which lead to difficulties and restrictions on the use of those processes. There are two notable technological barriers for single stroke shearing. First, the cutting quality is dependent on the cutting clearance, which scales with the thickness of the sheet material. This results in high demands on the positional tolerances and motion accuracy of the whole tool set-up and specifically the punch. For example, Joo et al. demonstrated that a machine vision system is necessary to accurately align punch and die plate in order to cut foils down to 25 µm thickness [2]. Second, the tools themselves have to meet very tight tolerances and the production of stamps and dies fit for micro shearing is still an active research topic [3].

One attempt to mitigate those problems is to substitute the stamp and apply the cutting force required for material separation by other means. Liu et al. for example used Nd:YAG laser-induced shock waves to cut foils of only 10 µm thickness [4]. This method was further developed towards an indirect laser shock process which uses a medium to transmit the force of the shock wave onto the workpiece. The medium could be a laser driven flyer [5] or a soft punch made of rubber material [6], which led to the fabrication of punched micro-gears using brass foils as thin as 20 µm [7]. However, a wavelength of 1.064 µm requires the use of an ablative layer as well as a confinement layer to create sufficiently strong laser shocks. The ablative layer has to be renewed after every pulse, which limits the speed of this process.

In this paper, we introduce a new laser shock punching process based upon pulsed TEA-CO_2-lasers. Using a

✉ H. Fenske
fenske@bias.de

[1] BIAS-Bremer Institut für angewandte Strahltechnik GmbH, Klagenfurter Str. 5, 28359 Bremen, Germany

[2] University of Bremen, 28359 Bremen, Germany

wavelength of 10.6 µm has the advantage that the creation of the laser-induced shock wave does not require any pre-treatments of the workpiece. Any laser pulse of sufficient energy density will immediately form a plasma above the surface of the workpiece which is opaque for the laser and absorbs most of the incoming radiation [8]. The use of TEA-CO_2 laser-induced shock waves for sheet metal forming has been shown first by Wielage et al. [9]. Meanwhile the realization of a mechanical joining process using the same laser set-up has been demonstrated by Veenas et al. [10]. and attempts to realise a laser shock shearing process were also reported [11]. However, those initial attempts still required multiple pulses to initiate a material separation. In this paper, the principle and influencing factors for single pulse laser shock punching are presented for the first time.

In order to initiate a shearing process, the force applied to the material has to be greater or equal to the cutting force. For laser shock punching the cutting force is transmitted by the pressure of a laser-induced shock wave. Accordingly, the force applied to the material depends on the size of the pressurized area. The force necessary to initiate material separation on the other hand depends on the length of the cutting path, as known from conventional cutting [12]. Therefore, the geometry of the cutting line should determine whether or not a material can be cut. This hypothesis will be investigated within this paper by examining the influence of the geometrical ratio of pressurized area to cutting path length.

2 Experimental set-up

2.1 Cutting process

Figure 1 depicts a schematic view of the experimental set-up for laser shock punching. It consists of three main components: the cutting die, the blank holder and the foil material, which is placed between the former two. The blank holder is made of polyoxymethylene. It has a drilled hole in the middle with a diameter of 3 mm and a height of 10 mm and is adjusted concentrically to the cutting die via positioning pins. Compressed air is blown onto the opening of the blank holder to ensure a constant and particle free atmosphere above the workpiece. The laser-induced shock wave is created using a TEA-CO_2-laser with a wave length of 10.6 µm, a pulse duration of 100 ns and a pulse energy of 6 J. The intensity distribution is flat-top and the beam profile is rectangular. The focus of the laser is set on the plane of the foil and the spot is adjusted concentrically to the centreline of the die/blank holder. The laser was set to single pulse mode and for every cutting attempt only one pulse was used.

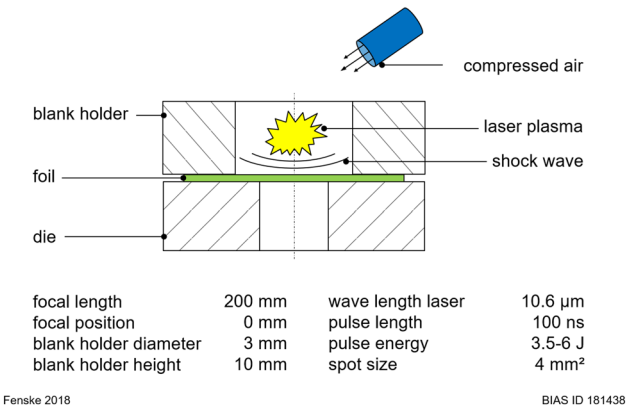

Fig. 1 Schematic view of the experimental set-up for laser shock punching

2.2 Manufacturing of cutting dies

Since standardized cutting dies were found to be unsuitable for the process, the manufacturing of own dies was undertaken. Circular cutting lines were made by drilling with subsequent reaming to improve the surface quality inside the drill hole. Gap- and square-shaped geometries were achieved by wire EDM. All custom-made dies were finished by subsequent grinding and polishing of the upper outer surface until they were mirror polished and no scratches were visible anymore to the naked eye. The cutting edge quality of the custom made dies was controlled using a SEM in secondary electron mode.

2.3 Variation of cutting line geometry

In Fig. 2 the geometrical ratio of pressurized area (A) to cutting path length (L) is derived for circular, gap- and square-shaped geometries. It is assumed, that all the foil material within the blank holder is homogeneously pressurized. To achieve an equal geometrical ratio A/L for all geometries, the size of the gap (b) has to be equal to the radius of the

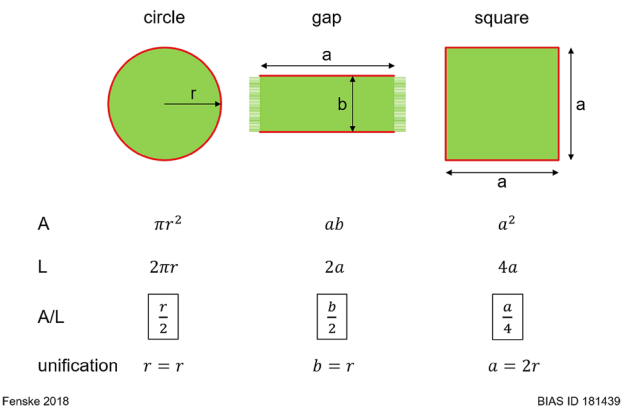

Fig. 2 Derivation of the geometrical ratio A/L

circle (r) and the side length of the square (a) has to be equal to the diameter of the circle (2r). The influence of the cutting line geometry on the cutting result was investigated by comparing all three geometries with the same geometrical ratio of 0.5 mm. Subsequently, the correlation of the foil thickness with the geometrical ratio was tested by determining the process window of aluminium foils for different geometrical ratios. For circular geometries, A/L ratios of 0.125–0.75 mm were examined (equals a change in radius from 0.25–3 mm). For gap-shaped geometries, A/L ratios of 0.25–1 mm were examined (equals a change in gap size of 0.5–2 mm). For all examined geometries, except for circular geometries at an A/L above 0.5 mm, the pressurized area is smaller than the spot size. The geometrical ratio of 0.75 mm is the upper limit for circular shaped geometries; at this point, the diameter of the circle is equivalent to the diameter of the blank holder drilling and any further increase in diameter would not result in an increase of pressurized area. We repeated the experiment using pulse energies of 4 J instead of 6 J respectively using brass foils instead of aluminium foils in order to examine the influence of pulse energy and material.

2.4 Properties and analysis of the foil material

Table 1 lists the key features of all foils used within this work. The data is presented as specified by the supplier of the respective foils. For the tensile strength the lower values generally corresponds to the lower thicknesses and the higher values correspond to the higher thicknesses. To investigate the influence of foil thickness on the morphology cut foils of 20–80 µm thickness were fixated and embedded for cross-sectional metallographic analysis. If not otherwise mentioned, all aluminium foils are in soft annealed condition (condition O). The influence of microstructure was investigated using 50 µm Al99.5 foil in work hardened condition (condition H18). Parts of this material were annealed at 600 °C for 100 h to create a very coarse grain structure. The microstructure of all 50 µm foils (work hardened, soft annealed and coarse grain annealed) was investigated by etching with Barker-solution. This was done on the rolled surface as well as in cross-section. The grain size was determined on the rolled surface using Olympus Stream Software following ASTM E112-12. Measurements were performed with the intercept method using a grid form with 5 bars horizontally and 5 bars vertically. Three micrographs for each annealing condition were measured and the results were averaged. The morphology of the cut edge for different annealing conditions was analysed in the SEM using the secondary electron detector.

3 Results

3.1 Cutting edge quality

In Fig. 3 SEM images of the cutting edge of a die complying with standard DIN 9845 form A can be seen in contrast to a SEM image of the cutting edge of a custom-made die. The extent of the edge area of the standardized die as seen in Fig. 3a is around 15 µm. However, the edge is very inhomogeneous and there are also areas in which material is jutting out over the edge (Fig. 3b). In contrast, the cutting edge area of the custom-made die is below 1 µm (Fig. 3c) and very homogeneous over the whole cutting path. All dies were freshly grinded and polished before every new experiment to achieve reliable cutting edge quality. This procedure results in a fresh and flawless new cutting edge.

3.2 Variation of cutting line geometry

The cutting results for circular, gap- and square-shaped cutting line geometries with the same geometrical ratio of 0.5 mm can be seen in Fig. 4a–c. Even though they exhibit very different sizes of pressurized area and cutting path length, they all cut the same 40 µm aluminium foil. For the circular and gap-shaped cutting line this displays the maximal cuttable foil thickness, while the square-shaped cutting line can even cut up to 50 µm. Under examination in the SEM the cut edge morphology along the circular and gap-shaped cutting lines was found to be equally good and

Table 1 List of all foil materials with their respective material composition, foil thickness, thickness tolerance and tensile strength as specified by the material supplier

Thickness (µm)	Material composition	Thickness tolerance	Tensile strength (MPa)
10, 30	AlFe1Si EN AW-8079	±8% of nominal thickness	75–95
20, 40, 50, 60, 70, 80	Al99.5 EN AW-1050A	±8% of nominal thickness	53–85
10	CuZn37 2.0321	±20% of nominal thickness	>450
20, 30	CuZn37 2.0321	±10% of nominal thickness	>450

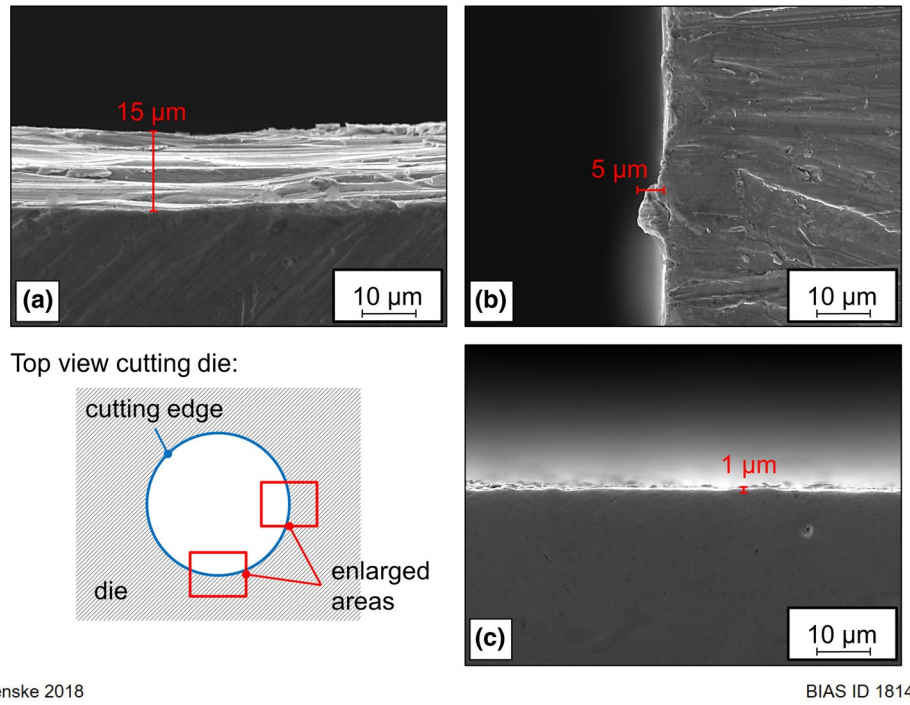

Fig. 3 SEM images of the cutting edge area of a standardized and a custom-made cutting die; **a, b** display different areas along the cutting edge of a die complying with standard DIN 9845 Form A while **c** displays the cutting edge of a custom-made die after polishing; all pictures are taken in top view, to determine the extent of the edge area

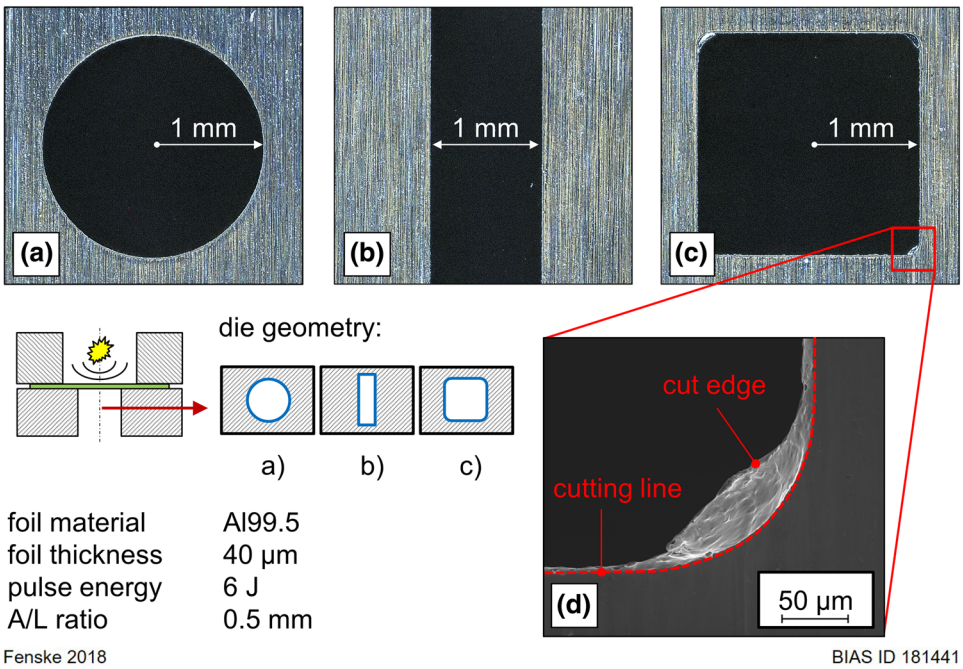

Fig. 4 Influence of different cutting line geometries with the same geometrical ratio A/L on the cutting quality of 40 µm aluminium foils; **a** foil cut with circular geometry, **b** foil cut with gap geometry, **c** foil cut with square geometry, **d** SEM image of the cutting quality in the corner region of the square geometry

homogeneous along the whole cutting path. The square-shaped geometry on the other hand does only exhibit a comparable cut edge quality along the middle of the sides and considerably worse cutting quality at the corners. In Fig. 4d a SEM image of a corner region can be seen. It is clearly visible that the foil was not cut along the cutting line but rather teared off within the pressurized area. The rounding of the cutting line is caused by the fabrication method because the sharpness of a corner produced by wire EDM is limited by the diameter of the wire.

3.3 Influence of foil thickness

Figure 5 depicts the process window for aluminium foils in dependence of the geometrical ratio A/L for circular and gap-shaped cutting line geometries. At least ten cutting attempts

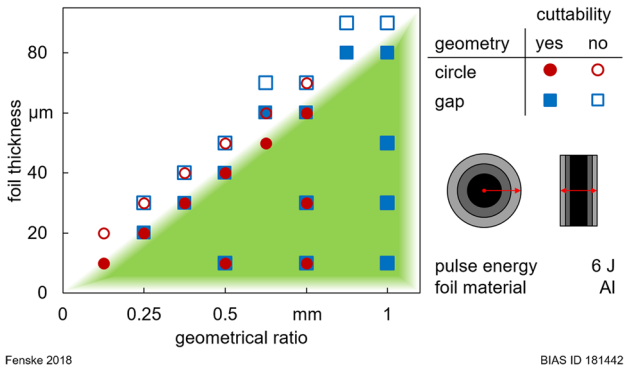

Fig. 5 Process window of cuttable foil thickness in dependence of the geometrical ratio A/L; the examined ratios vary depending on the geometry of the cutting line (circular: 0.125–0.75 mm; gap-shaped: 0.25–1 mm)

were performed for each data point. A foil thickness was determined to be cuttable by a certain geometrical ratio if every cutting attempt resulted in a cut. The maximal cuttable thicknesses for the circular cutting line geometry can be fitted to a straight line with a slope of 80 µm/mm. The gap-shaped geometries deviate from this line at some points, reaching higher cuttable thicknesses at geometrical ratio 0.625 mm and 0.875 mm, but overall follow the same trend. Generally each thickness below this threshold can also be cut, as indicated by the green area. No results for square-shaped geometries are included, because it was not possible to achieve good cutting quality along the whole cutting line for those geometries.

Fig. 6 shows a metallographic cross section of an 80 µm foil cut with gap-shaped cutting line geometry at a geometrical ratio of 1 mm. An enlargement of the cut edge is displayed in Fig. 6a. The morphology of the cut edge is representative for all foil thicknesses. Characteristic values are: an edge rounding that is roughly as long as the foil thickness and a burr length of 10–20% of the foil thickness. The burr displays a tip shaped ending. An equivalent narrowing can be seen on the side of the slug (Fig. 6b). Furthermore, a significant necking can be found within the pressurized area (Fig. 6c). In the area with the strongest reduction, the foil thickness decreases to only 30 µm.

3.4 Influence of pulse energy and material

Figure 7 shows an extension of the experiment depicted in Fig. 5. Only the maximal cuttable foil thickness is plotted. The results for aluminium foils cut with 6 J pulse energy are complemented by the results achieved when using 4 J pulse energy as well as when using brass foils instead of aluminium foils. Both data sets also exhibit a linear dependency of the maximal cuttable foil thickness with the geometrical ratio A/L, but their respective slope is lower. With around 60 µm/mm the slope for aluminium foils cut with 4 J is at only 75% of the slope of the same foils cut with 6 J pulse energy. The slope of the brass foils cut with 6 J pulse energy on the other hand is roughly 30 µm/mm and thus approximately one-third of the slope of the aluminium foils cut with the same pulse energy.

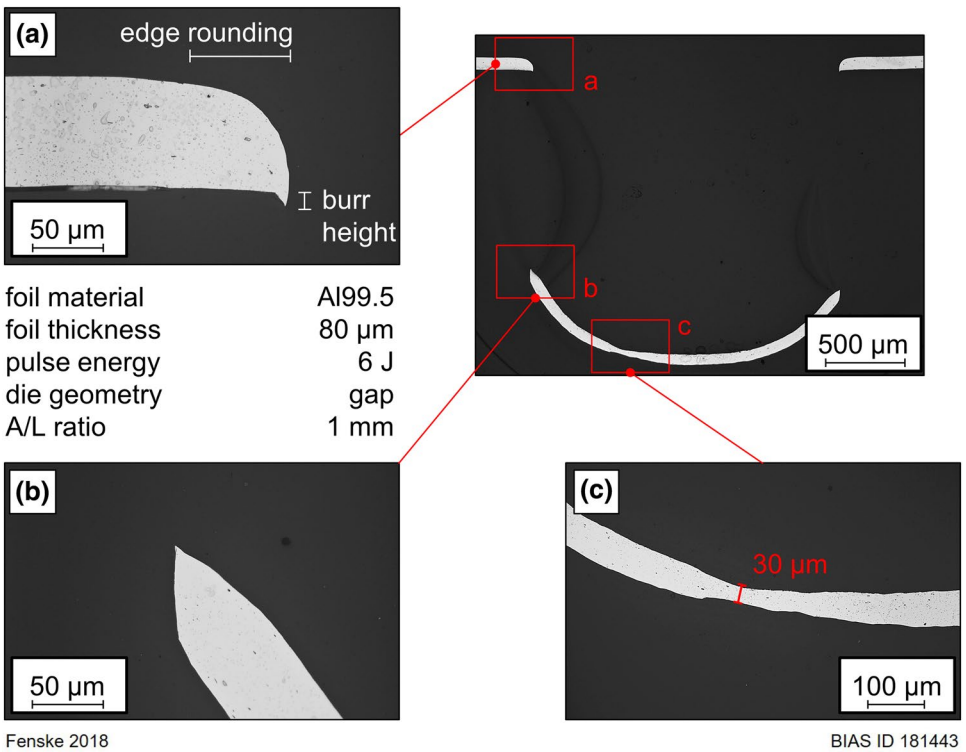

Fig. 6 Metallographic cross section of an 80 µm aluminium foil cut with gap-shaped cutting line geometry at an geometrical ratio A/L of 1 mm; **a** enlargement of the cut edge area, **b** enlargement of the cut edge on the side of the slug, **c** enlargement of the area with the strongest necking within the slug

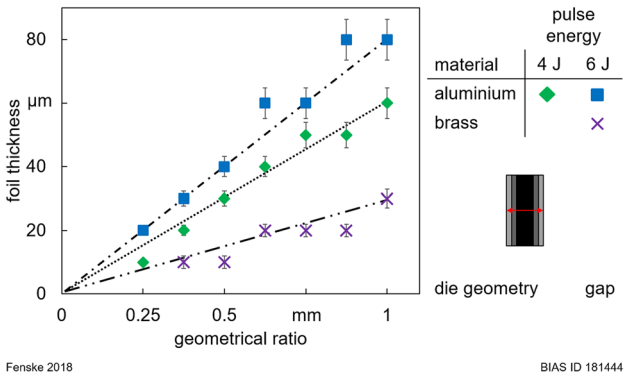

Fig. 7 Maximal cuttable foil thickness plotted over the geometrical ratio A/L for gap-shaped cutting line geometries using varying pulse energies and foil material; the dotted lines indicate slopes of 80/60/30 µm/mm; the error bars indicate the variations in the foil thickness

3.5 Influence of microstructure

The influence of the microstructure on the cutting result was exemplary investigated using aluminium foils with 50 µm thickness. Figure 8 shows the grain structure of the foils under three different annealing conditions: work hardened, soft annealed and coarse grain annealed. The results of the grain size measurement performed on the rolled surfaces are presented in Table 2. The average line cut length is taken to be roughly equivalent to the average grain size. By this definition the average grain size of the soft annealed foils was significantly smaller than the foil thickness, while the average grain size of the coarse grain annealed foils was significantly bigger than the foil thickness. This difference can also be seen in the etched cross sections of the foils. For the soft annealed foil (Fig. 8b), there are at least 4–5 grains over the foils' thickness, contrary to the coarse grain annealed foils (Fig. 8c) which only exhibit 1–2 grains over the foils' thickness. No grain sizes could be determined for the work hardened foil because they exhibit a very strong texture. Nevertheless, a multitude of grains are clearly visible over the foils' thickness, see the etched cross section in Fig. 8a.

Table 2 Results of the grain size measurement

Annealing condition	ASTM grain size number	Average line cut length (d, µm)	Foil thickness (s, µm)	Ratio s/d
Soft annealed	7	29	50	1.7
Coarse grain annealed	4.3	75	50	0.7

The influence of the microstructure on the cutting result is illustrated in Fig. 9. All foils were cut using circular cutting line geometry. The foils were cut at different geometrical ratios of 0.75 mm, 0.625 mm and 0.5 mm for the work hardened, soft annealed and coarse grain annealed condition respectively. These are the lowest geometrical ratios with which the corresponding foils can be cut. At the upper half of Fig. 9, the cut edge morphologies resulting from the different annealing conditions are depicted. None of the foils display signs of fracture, which indicates a high amount of plastic deformation prior to the material failure. The work hardened foil (Fig. 9a) generally only forms a very small burr which looks almost aligned with the lower side of the

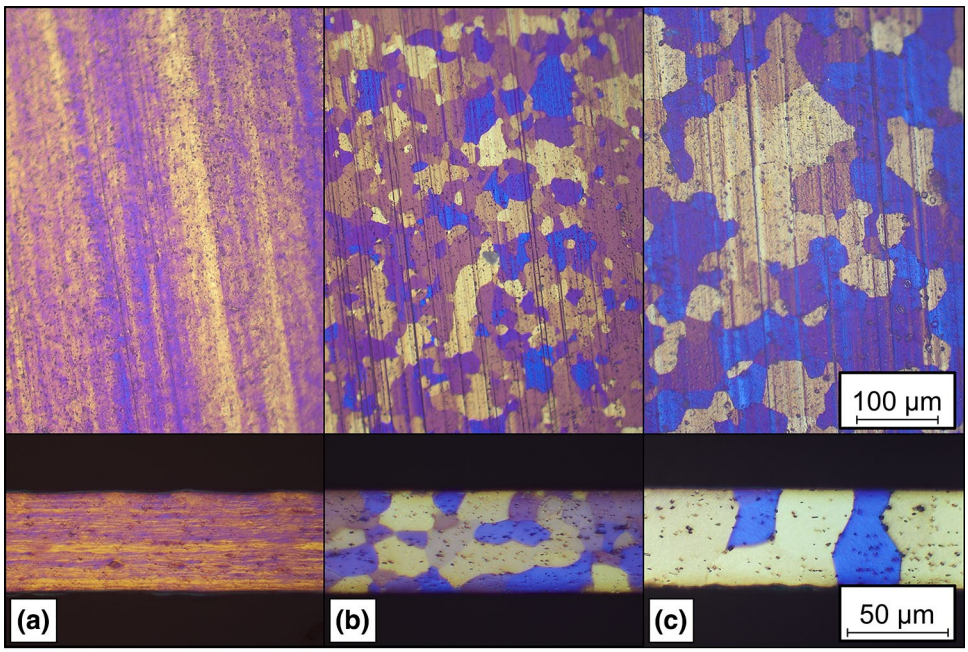

Fig. 8 Grain structure of the rolled surface (on top) and in cross section (below) for 50 µm aluminium foils in **a** work hardened, **b** soft annealed and **c** coarse grain annealed condition

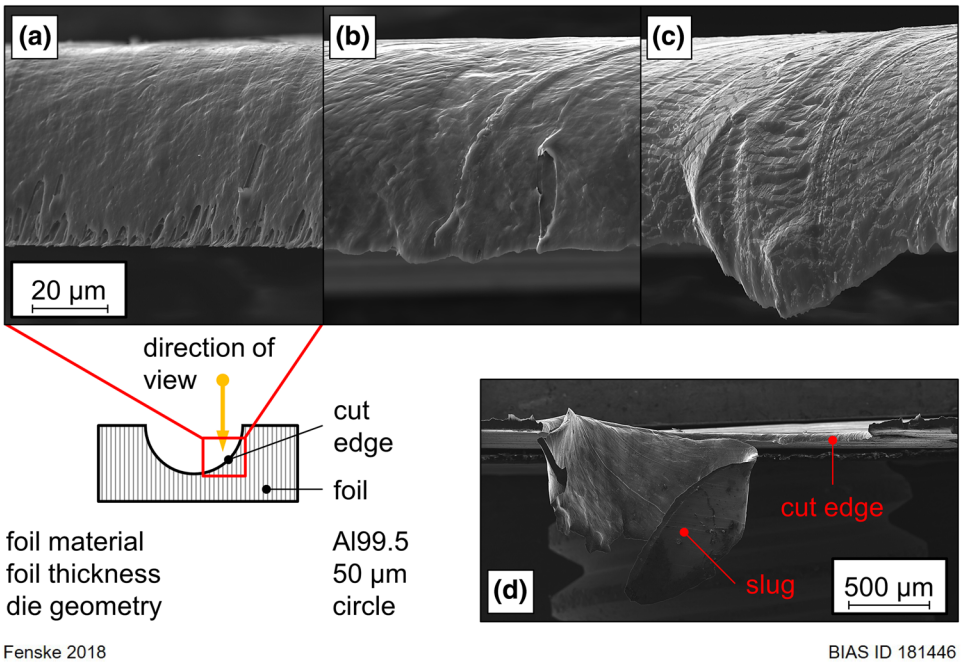

Fig. 9 SEM image of the cutting edge morphology of 50 µm aluminium foils in **a** work hardened, **b** soft annealed and **c** coarse grain annealed condition; **d** overview of an incomplete cutting often found for coarse grain annealed foils; all foils were cut with circular cutting line geometry and bisected prior to examination

foil. At higher magnifications, however, it is visible that it actually consists of many small tips. The soft annealed foil (Fig. 9b) already shows a bigger and more inhomogeneous burr formation where the length of the burr does vary locally. The coarse grain annealed foil (Fig. 9c) continues the trend and exhibits a very strong, but also highly inhomogeneous burr formation which takes the form of local spikes with a width in the dimension of the foil thickness. The cracks that can be seen on the cut surface of the coarse grain annealed foils are not cracks within the aluminium material, but rather cracks of the thick oxide layer which formed during the annealing process. Figure 9d shows an incompletely cut coarse grain annealed foil where the slug still adheres to the rest of the foil. Incomplete cutting is a common occurrence for foils in this annealing condition.

4 Discussion

The SEM analysis of the cutting edge area displays an insufficient cutting edge quality of the standardized die. This explains why no cutting could be realised with it. Even though still available for purchase, the German standard DIN 9845 has been revoked already and was replaced by the international standard ISO 8977. However, neither does regulate the geometrical dimensions of the cutting edge. Instead, they only dictate the surface quality of the outer and inner surface adjacent to the cutting edge. While DIN 9845 commands a maximal outer surface roughness of $R_z = 6.3$ µm [13], ISO 8977 proclaims a threshold of $R_a = 1.6$ µm [14]. Both specifications seem unsuitable to ensure a cutting edge quality that is fit for the cutting of foils in the micrometre range. In contrast, the custom-made cutting dies, with an edge area of less than 1 µm, showed good results for foils down to 10 µm thickness. Thus it can be concluded, that even though standardised dies are not suitable for laser shock punching, cutting dies with adequate cutting edge quality can be produced using simple manufacturing techniques such as drilling or wire EDM and subsequent polishing of the upper outer surface.

The cutting experiments with the custom-made dies clearly show that the geometrical ratio of pressurized area (A) to cutting path length (L) is an important parameter for laser shock punching. This can be explained by a balance of forces between the force applied onto the foil F_p by the pressure of the laser shock p, see Eq. (1), and the cutting force F_c needed for material separation, see Eq. (2). For simplicity, it is assumed that all the foil material is homogeneously pressurized.

$$F_p = p \cdot A \tag{1}$$

$$F_c = L \cdot s \cdot k_c \tag{2}$$

Equation (2) is known from conventional cutting [12]; s is the foil thickness, while k_c is a material specific constant depending on the tensile strength. Cutting is assumed to happen if $F_p \geq F_c$. Equating (1) and (2) and changing the result to s leads to:

$$s \leq \frac{A}{L} \cdot \frac{p}{k_c} \tag{3}$$

Equation (3) predicts that under the condition of constant pressure and material, the cuttability of a certain foil thickness is determined only by the ratio A/L of the desired cutting line geometry. However, the investigated square-shaped geometry did not show a sufficient cutting result, as opposed to its circular and gap-shaped counterparts. This is likely a consequence of an inhomogeneous stress distribution along the cutting line. Homogeneously pressurized square-shaped geometries exhibit a stress concentration on the middle of the sides. Accordingly, the material separation starts at these locations and propagates from there on to the corners. This leads to a changing direction of force along the cutting line, which ultimately leads to a tearing of the foil within the pressurized area instead of the desired separation along the cutting edge. A homogeneous stress distribution along the cutting line is therefore a necessary condition to achieve good cutting results.

Equation (3) can also be interpreted as a linear function, where the maximal cuttable foil thickness is plotted against the geometrical ratio A/L (again, under the condition of constant pressure and material). Indeed, a respective trend can be clearly observed in the examined process window for circular and gap-shaped geometries. Even circular geometries whose pressurized areas are slightly bigger than the laser spot size (namely circular geometries of $A/L > 0.5$ mm) display no significant deviation from the linear trend. Consequently, the initial assumption that all of the foil material is homogeneously pressurized seemingly holds true. This suggests a smooth decrease in pressure around the laser spot, which is compliant with the characteristics of TEA-CO_2 laser-induced shock waves [10].

Furthermore, Eq. (3) predicts the slope of this linear correlation to be proportional to the pressure of the laser-induced shock wave and inversely proportional to the material constant k_c. Both predictions were examined qualitatively by varying pulse energy and foil material. The pulse energy correlates with the pressure of the laser-induced shockwave [15] and consequently a decrease in pulse energy led to a decrease of the slope. The material constant k_c on the other hand correlates with the tensile strength of the cut material [12] and accordingly the use of brass foil led to a decrease of the slope as well. However, the correlation is not linear. The tensile strength of the brass foils used for this experiment is at least five to eight times as high as the one of the aluminium foils, but the difference in slope is only by the factor of 3. Indeed, it is unknown so far if tensile strength is the relevant material parameter for laser shock punching, even though the morphology of the cut edge exhibits a strong resemblance of the characteristic necking behaviour known from plastic tensile failure.

In summary, the experimental data strongly support the validity of Eq. (3). The equation successfully predicts qualitative trends for the cuttability of different foil thicknesses and foil materials depending on the geometrical ratio of the cutting line geometry and the pulse energy. However, quantitative calculations about the cuttability of different foil materials are not possible to date. The correlation of foil thickness to the geometrical ratio nevertheless allows for an easy determination of process limits by gathering only small amounts of experimental data.

The microstructure of the foil material is another fundamentally important factor for laser shock punching. Work hardened foils show the smallest and most regular burr formation, but also require a higher geometrical ratio to be cut. This is consistent with the results discussed above, because the work hardened foils exhibit a higher tensile strength compared to the other annealing conditions. The soft annealed foils on the other hand display first signs of a locally varying burr height. The edge morphology of the coarse grain annealed foils continues the trend, displaying a strongly varying burr height, which take the form of local spikes that protrude from the cutting edge. This is a strong sign for a single grain effect. If the grain size becomes big in comparison to the foil thickness, this results in anisotropic material properties along the cutting line. This in turn leads to an anisotropic cutting behaviour, which explains the observed inhomogeneous burr formation. Additionally, the examined coarse grain annealed foils tended to display incomplete cutting. Some even ruptured within the pressurized area before any material separation happened along the cutting line. This highlights an important characteristic of the process: the material within the pressurized area has to be strong enough to transmit the forces applied onto it. Material defects like areas that tear easier than the rest of the foil due to anisotropic material behaviour limit the applicability of the process.

5 Conclusion

Contrary to conventional punching, in laser shock punching the cutting force is transmitted via the pressure surge of a laser-induced shock wave and not by the movement of a cutting stamp. This leads to unique process characteristics, which were described here for the first time. Because the process is designated to cut foils in the micrometre range, size effects are important for the process.

The findings presented in this work are summarized in the following:

- For laser shock punching it is important to have a good and homogeneous cutting edge quality, which is sharp in relation to the foil thickness. Cutting dies complying with the current standards are not suitable.

- Under otherwise constant conditions, the cuttability of a certain cutting line geometry depends on the geometrical ratio of pressurized area to cutting path length.
- However, a good cutting result can only be achieved for geometries where a homogeneous stress distribution along the cutting line is present, which was demonstrated for circular and gap-shaped geometries in contrast to a square-shaped cutting line.
- The maximal cuttable foil thickness scales linearly with the described geometrical ratio. First experiments indicate that the slope of the line depends on the pressure level of the laser-induced shock wave as well as on the strength of the foil material.
- The microstructure of the foil material has a significant impact on the cutting quality. If the average grain size is greater than the thickness of the foil, an increased and inhomogeneous burr formation can be observed and there is a high risk of incomplete cutting due to premature rupture within the pressurized area.

Acknowledgements The financial support of the project "Schneiden durch laserinduzierte Schockwellen" (Project number 289438332) by the German Research Foundation (DFG) is gratefully acknowledged.

References

1. Vollertsen F, Biermann D, Hansen HN, Jawahir IS, Kuzman K (2009) Size effects in manufacturing of metallic components. CIRP Ann Manuf Technol 58(2):566–587
2. Joo BY, Rhim SH, Oh SI (2005) Micro-hole fabrication by mechanical punching process. J Mater Process Technol 170(3):593–601
3. Zeng Z, Li D, Yu Z, Yang X, Li J, Kang R (2018) Study of machining accuracy of micro punching mold using micro-EDM. Procedia CIRP 68:588–593
4. Liu H, Shen Z, Wang X, Wang H, Tao M (2010) Numerical simulation and experimentation of a novel micro scale laser high speed punching. Int J Mach Tools Manuf 50(5):491–494
5. Liu H, Wang H, Shen Z, Huang Z, Li W, Zheng Y, Wang X (2012) The research on micro-punching by laser-driven flyer. Int J Mach Tools Manuf 54:18–24
6. Liu H, Lu M, Wang X, Shen Z, Gu C, Gu Y (2015) Micro-punching of aluminum foil by laser dynamic flexible punching process. Int J Mater Form 8(2):183–196
7. Li J, Liu H, Shen Z, Qian Q, Zhang H, Wang X (2016) Formability of micro-gears fabrication in laser dynamic flexible punching. J Mater Process Technol 234:131–142
8. Barchukov AI, Bunkin FV, Konov VI, Lyubin AA (1974) Investigation of lowthreshold gas breakdown near solid targets by CO2-laser radiation. Zh Eksp Teor Fiz 66:965–982
9. Wielage H, Schulze Niehoff H, Vollertsen F (2008) Forming behaviour in laser shock deep drawing. In: International conference on high speed forming
10. Veenaas S, Wielage H, Vollertsen F (2014) Joining by laser shock forming: realization and acting pressures. Prod Eng Res Devel 8(3):283–290
11. Veenaas S, Vollertsen F (2015) Areas of application for TEA CO_2-laser induced shock waves. In: International WLT-conference on lasers in manufacturing, vol 8, pp 1–10
12. Kolbe M, Hellwig W (2015) Spanlose Fertigung Stanzen. Springer Fachmedien, Wiesbaden, p 28
13. DIN 9845:1979-02, Schneidbuchsen und Stempelführungsbuchsen
14. DIN ISO 8977:2003-10, Werkzeuge der Stanztechnik - Schneidbuchsen (ISO 8977:2003)
15. Wielage M (2011) Hochgeschwindigkeitsumformen durch laserinduzierte Schockwellen. Dissertation, Universität Bremen, p 53